DEVELOPMENTAL BIOLOGY 175, 283–300 (1996)
ARTICLE NO. 0115

Interactions between Melanophores and the Lateral Lines That Generate Stripes in the Salamander *Ambystoma tigrinum tigrinum* (Ambystomatidae)

David M. Parichy

Section of Evolution and Ecology and The Center for Population Biology, University of California at Davis, Davis, California 95616

A prominent element of the early larval pigment pattern in the salamander *Ambystoma tigrinum tigrinum* (family Ambystomatidae) is a horizontal stripe over the lateral surface of the myotomes where otherwise abundant, neural crest-derived melanophores are not found. This study examines the formation of this ''melanophore-free region.'' When the trunk lateral lines were ablated (by removing cranial lateral line placodes), the melanophore-free region did not form; instead, melanophores populated the middle of the flank and the distribution of yellow, neural crest-derived xanthophores was perturbed. Time-lapse videomicrography demonstrated that during normal development, the melanophore-free region is established because melanophores retreat from the midbody lateral line primordium as it migrates caudally along the inner side of the epidermis. Melanophores do not repopulate the middle of the flank after primordium migration and heterochronic grafting experiments suggest that extracellular factors contribute to maintaining the melanophore-free region during these later stages. Finally, photographic series, microsurgical manipulations, electron microscopy, and staining for molecules of the extracellular matrix (peanut agglutinin-binding components, tenascin, chondroitin sulfate proteoglycans, fibronectin, laminin) suggest that several factors contribute to establishing and maintaining the melanophore-free region, including steric effects of the lateral lines, interactions between melanophores and xanthophores, lateral line-dependent alterations of the subepidermal basement membrane, and a general elaboration of the extracellular matrix. Lateral line effects on melanophores are inferred to be a shared, ancestral feature of pigment pattern development for the families Ambystomatidae and Salamandridae (D. M. Parichy, *Dev. Biol.* 174, 265–282. 1996). The results of this study thus provide insights into a phylogenetically primitive mechanism for stripe formation, and a context for interpreting evolutionary innovations in pattern-forming mechanisms.

INTRODUCTION

The vertebrate neural crest is a transient population of cells that arises shortly after neurulation along the dorsal neural tube (reviewed in Hall and Hörstadius, 1988; Epperlein and Löfberg, 1993; Erickson and Perris, 1993; Selleck *et al.*, 1993; Bronner-Fraser, 1994). From this position, neural crest cells disperse widely and contribute to numerous tissues and organs, including the peripheral nervous system, endocrine glands, and fin mesenchyme, as well as such phylogenetically variable characters as the teeth and bones of the craniofacial skeleton, and externally visible pigment patterns (e.g., DuShane, 1934; Detwiler, 1937; Bronner-Fraser and Fraser, 1989; Collazo *et al.*, 1993; Couly *et al.*, 1993; Raible and Eisen, 1994; Serbedzija *et al.*, 1994; Smith *et al.*, 1994). A fuller understanding of vertebrate diversity thus requires an understanding of the mechanisms that pattern neural crest derivatives and how these mechanisms evolve. An important step toward this goal is to identify shared, ancestral patterning mechanisms, because they provide insights into phylogenetically primitive modes of development, and a context for interpreting evolutionary innovations.

Salamander pigment patterns are a useful model system for studying the development and evolution of neural crest derivatives. Shortly after hatching, these patterns result principally from the numbers and spatial arrangements of two types of pigment cells, or chromatophores: black melanophores and yellow xanthophores (reviewed in Epperlein and Löfberg, 1993; Erickson, 1993). A distinctive and phylogenetically common element of early larval patterns is a region over the lateral face of the myotomes that is rela-

0012-1606/96 $18.00

tively free of melanophores (reviewed in Parichy, 1996a; see below). Such ''melanophore-free regions'' are typically populated by xanthophores and bordered by melanophores both dorsally and ventrally, so the overall pattern consists of a light horizontal stripe between dark concentrations of melanophores.

Formation of melanophore-free regions can depend on the lateral line sensory system (Parichy, 1996b). The trunk lateral lines of fishes and aquatic amphibians detect mechanical stimuli via neuromasts located at periodic intervals in the integument (Stone, 1933, 1938; Winklbauer, 1989; Northcutt, 1992; Collazo *et al.*, 1994). In salamanders, three trunk lateral lines arise bilaterally from postotic, ectodermal placodes in the head, which deploy in sequence midbody, dorsal, and ventral lateral line ''primordia.'' These primordia migrate caudally along the inner side of the epidermis and are followed by extending neurites of the lateral line nerves. As the primordia migrate, they deposit clusters of cells that later erupt through the epidermis as mature neuromasts (Smith *et al.*, 1990; Northcutt *et al.*, 1994, 1995).

In the salamander *Ambystoma tigrinum tigrinum* (family Ambystomatidae), melanophores at first scatter uniformly over the somites, whereas xanthophores are found in aggregates dorsal to the neural tube. As xanthophores disperse, melanophores recede short distances to form a series of alternating ''vertical bars'' over the dorsal myotomes (Olsson and Löfberg, 1992; Parichy, 1996b; also see Lehman, 1957; Epperlein and Löfberg, 1990). Meanwhile, a subtle melanophore-free region appears over the middle of the myotomes in the vicinity of the midbody lateral line primordium (Parichy, 1996b). During later development, the melanophore-free region persists and becomes increasingly distinctive. If lateral line development is prevented, however, a more uniform distribution of melanophores is found in *A. t. tigrinum*, as well as seven of eight other taxa examined. Based on these and other findings, lateral line effects on melanophores were inferred to be a shared, ancestral feature of pigment pattern development for the families Ambystomatidae and Salamandridae, which can generate melanophore-free regions in extant taxa, and also conferred the potential for such patterns in a common ambystomatid–salamandrid ancestor.

This study demonstrates that in *A. t. tigrinum*, melanophores actively evacuate the middle of the flank in response to the lateral line primordium, whereas extracellular factors can inhibit melanophores from populating the middle of the flank during later development. Evidence is then presented that suggests patterning roles for steric effects of the lateral lines, interactions between melanophores and xanthophores, and lateral line-dependent and -independent alterations to the extracellular matrix (ECM).[1] These findings provide insights into primitive mechanisms for stripe formation and set the stage for investigations into evolutionarily derived pattern-forming mechanisms.

[1] Abbreviations used: ECM, extracellular matrix; HSS, Hepes-buffered Steinberg's solution; PNA, peanut agglutinin lectin; SEM, scanning electron microscopy; TEM, transmission electron microscopy.

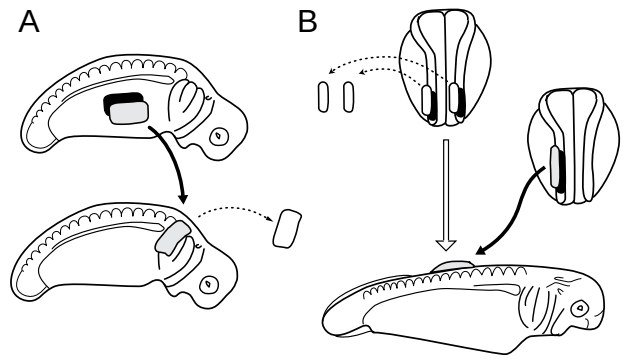

FIG. 1. Microsurgical manipulations used in this study. (A) Prevention of lateral line development by replacing placode-area ectoderm with belly epidermis. (B) Behavior of younger melanophores in older host embryos: DiI-labeled neural folds containing prospective neural crest cells were grafted to the dorsal neural tube of developmentally more advanced, neural crest-depleted hosts.

MATERIALS AND METHODS

Embryos, Rearing Conditions, and Staging

Ambystoma t. tigrinum embryos were obtained from natural populations (Charles Sullivan Co., Nashville, TN; K. Mierzwa, Cook County, IL) and were maintained in 20% Hepes-buffered Steinberg's solution (HSS; Asashima *et al.*, 1989; plus 37.5 IU/ml penicillin, 37.5 μg/ml streptomycin) at 9–15°C. Staging followed Bordzilovskaya *et al.* (1989) for the closely related *A. mexicanum* (Shaffer, 1993) and all stage numbers are preceded by a ''B.''

Embryological Manipulations and Quantitation

General microsurgical procedures, vital labeling, and quantitation of chromatophore positions followed Parichy (1996b). Lateral line development was prevented by replacing lateral line placode-area ectoderm (Northcutt *et al.*, 1994, 1995) unilaterally with belly epidermis from a similarly staged donor (Fig. 1A). The side for lateral line ablation was chosen randomly for each embryo. Additionally, heterochronic chimeras were used to examine the factors that maintain the melanophore-free region (Fig. 1B). Single DiI-labeled neural folds (containing prospective neural crest cells) were dissected from B15/16 donors and grafted to slits made in the epidermis dorsal to the neural tube of B32/33 hosts. To minimize potentially confounding effects of increased total chromatophore densities, hosts were used that had been depleted of endogenous chromatophores by removing portions of the trunk neural folds at B15/16. Chimeras were allowed to develop past B43 (when a definitive early larval pattern normally would be formed), and then were photographed under brightfield, FITC, and RITC illumination to identify melanophores, xanthophores, and DiI-labeling, respectively.

Time-Lapse Videomicrography

Time-lapse videos were used to observe interactions between melanophores and the midbody lateral line primordium. To enhance the visibility of the primordium, lateral line placode-area ectoderm was stained with Nile blue sulfate (Stone, 1933). Embryos (B35–36) were placed in agar-lined dishes containing 20% HSS and 0.005% benzocaine as an anesthetic and videos were recorded for 6–12 hr using a Panasonic time-lapse video recorder (1:140 hr) and Sony CCD video camera mounted on a Leitz Diaplan microscope. Responses of individual melanophores that contacted the distal tip of the lateral line primordium were quantified by measuring the final dorsoventral distances of these cells from the center of the lateral line (there is little curvature of the flank in the immediate vicinity of the lateral line, where melanophore movements were examined). Analysis of covariance then was used to normalize these absolute distances according to the length of time that cells were observed after contacting the primordium.

Photographic Series, Shape Changes, Lateral Line Velocity, and Location

Interactions among melanophores, xanthophores, and the lateral lines also were examined in photographic series of individual embryos in which the lateral lines had been labeled with DiI (see Parichy, 1996b). To examine shape changes of the flank relative to lateral line development, the distance between the dorsal and ventral margins of individual myotomes in the middle of the trunk was measured from the first appearance of externally visible melanophores (B35) through formation of the early larval pigment pattern (B42). To calculate the average velocity of the midbody lateral line primordium within each embryo, the displacement of the distal tip of the primordium was measured every 3 hr for 9–18 hr, using centers of xanthophore dispersal as landmarks. Such measurements provide reasonable estimates of primordium velocity because anteroposterior expansion of the flank is minimal in the immediate vicinity of the primordium tip (data not shown). To identify the midbody lateral line nerve in transverse sections, larvae with DiI-labeled lateral lines were fixed in 4% paraformaldehyde, embedded in gelatin, sectioned at 20 μm on a Bright cryostat, and viewed under RITC illumination.

Transmission Electron Microscopy

Transmission electron microscopy (TEM) was used to examine the subepidermal basement membrane. Embryos were fixed for 30 min in 2.5% glutaraldehyde/1.0% paraformaldehyde/2.5% DMSO in 0.05 *M* Pipes at room temperature, then were cut transversely and placed in fresh fixative overnight at 4°C. After washing in Pipes, embryos were dehydrated in ethanol, transferred to propylene oxide, and embedded in EPON-Araldite. Embryos were then thick sectioned at 5 μm, and sections of interest were reembedded and thin sectioned in the gold interference range. After staining with uranyl acetate and lead citrate, specimens were viewed in a Philips 401 transmission electron microscope.

Scanning Electron Microscopy

Scanning electron microscopy (SEM) was used to examine physical relationships of the lateral lines with surrounding tissues. Most embryos were fixed and dehydrated in ethanol, as for TEM, and then were critical point dried and sputter coated with gold. Alternatively, freeze-substituted, paraffin-embedded specimens (below) were first sectioned to the middle of the trunk. The remaining, unsectioned tissue was then deparaffinized in xylene, rinsed in 100% ethanol, critical point dried, and sputter coated. All specimens were viewed in a Philips 501 scanning electron microscope and chromatophores were identified by comparison with photographs taken prior to SEM preparation.

Immunohistochemistry and Histochemistry

Antibody staining and lectin histochemistry were used to examine the distributions of ECM components in embryos prepared by freeze substitution (Bronner-Fraser and Fraser, 1989). Embryos were chilled to 4°C, immersed (ca. 1 sec) in ice-cold 95% methanol, and then frozen in isopentane chilled over liquid N_2 (30 sec). Embryos were then transferred to vials containing N_2-chilled 100% methanol and placed at −80°C. After 24 hr, the freeze substitution medium was replaced with fresh −80°C 100% methanol and left for an additional 48 hr. Vials were then transferred to −20°C for 24 hr, 4°C overnight, and room temperature for 2–3 hr. Embryos were then rinsed in 100% methanol, cleared in xylene, embedded in Paraplast X-tra, and sectioned at 12 μm. For each embryo, 10 sections each from the anterior, middle, and posterior trunk were mounted per slide, and for each ECM component, several embryos representing multiple stages were stained simultaneously. Slides were deparaffinized and rehydrated in ethanol, rinsed in phosphate-buffered saline (PBS), and blocked in 0.1% bovine serum albumin/PBS. Sections were incubated with primary antibody for 18 hr at 4°C, washed in PBS, then incubated with the appropriate RITC-conjugated secondary antibody (Cappel) for 1.5 hr at room temperature. Sections then were washed and coverslipped with an antifade mounting medium. Fluorescein-conjugated peanut agglutinin lectin (PNA; Vector) was used according to Oakley *et al.* (1994). For each ECM component, sections were photographed (Kodak Tri-X film) using identical exposures and comparisons were made only within rounds of staining (not across days or trials).

A polyclonal antiserum against *Xenopus laevis* tenascin from XTC cells (Riou *et al.,* 1991; Caubit *et al.,* 1994) was provided by Dr. J.-F. Riou. Monoclonal antibody (mAb) M1 against chicken tenascin-C (myotendinous antigen; Chiquet and Fambrough, 1984) was provided by Dr. R. P. Tucker. Monoclonal antibodies CS-56 against chondroitin-4 and -6 sulfate (Avnur and Geiger, 1984; Sigma) and ΔDi-6S (Couchman *et al.,* 1984; ICN) were used to examine the distribution of chondroitin sulfate proteoglycans (for mAb ΔDi-6S, sections were pretreated with 0.2 U/ml Calbiochem chondroitinase ABC for 1 hr at 37°C; extensive digestion abolished staining with mAb CS-56). A polyclonal antibody against *A. mexicanum* plasma fibronectin (Boucaut and Darribère, 1983; Boucaut *et al.,* 1984) was a gift of Dr. T. Darribère and a polyclonal antiserum against mouse laminin was provided by Dr. H. K. Kleinman (tested with and without collagenase pretreatment, which enhanced staining slightly but did not yield qualitatively different results). For all rounds of staining, control sections were treated identically except for omission of the primary reagent.

RESULTS

Distributions of Melanophores and Xanthophores

The early larval pigment pattern of *A. t. tigrinum* consists of alternating vertical bars over the dorsal myotomes and a melanophore-free region over the middle of

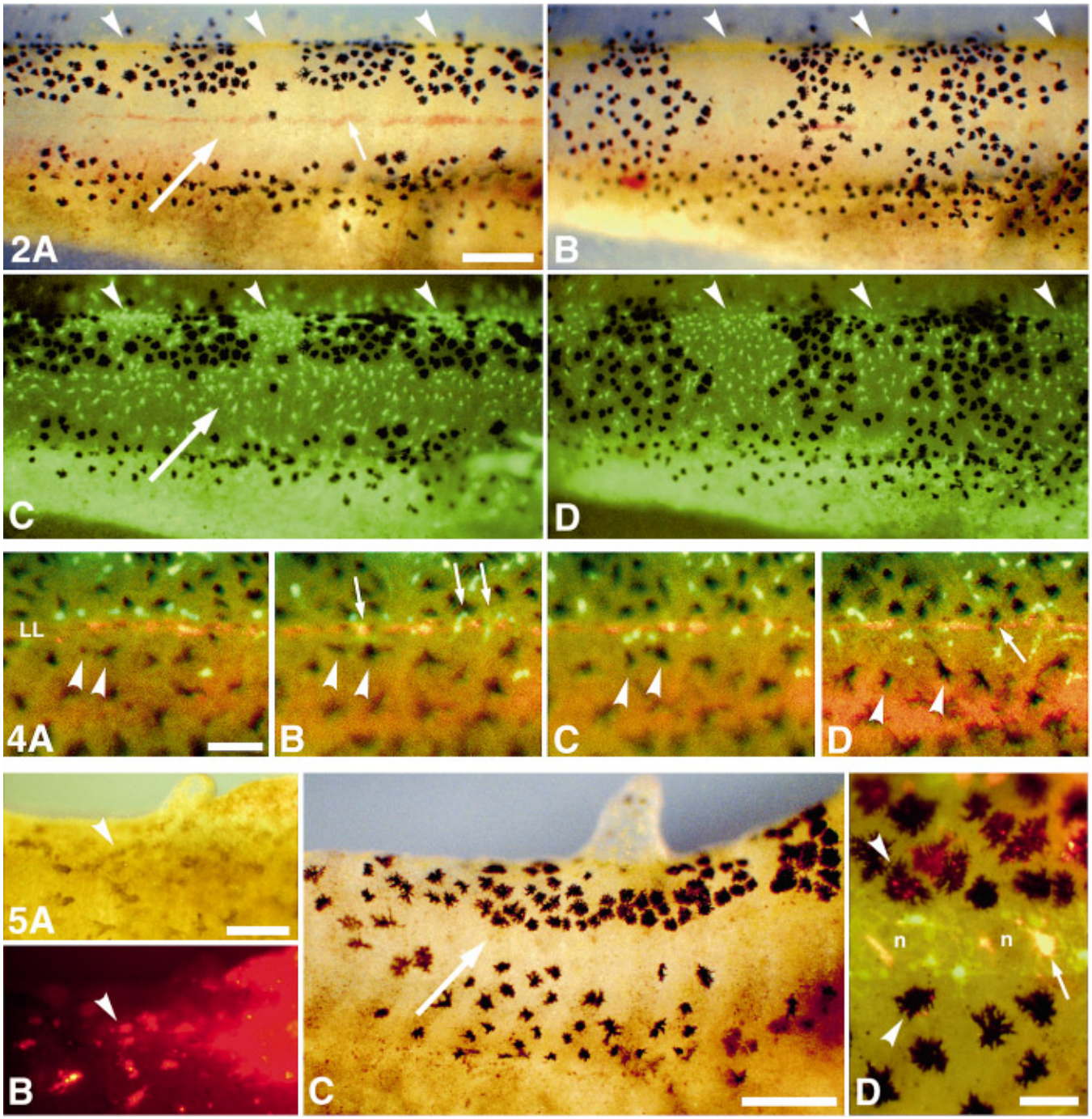

FIG. 2. Ablation of the lateral lines alters both melanophore and xanthophore distributions. Brightfield views (A, B) show melanophores and epifluorescent views (C, D) reveal xanthophores on opposite sides of a single individual (B42). Images in B and D are reversed left–right to facilitate comparison with A and C. Anterior is to the right. (A, C) A distinctive melanophore-free region (large arrow) is present in the middle of the flank and is colonized by xanthophores on the unmanipulated side of a representative larva. Small arrow in A indicates a subcutaneous artery that runs along the lateral face of the myotomes, immediately ventral to the midbody lateral line. (B, D) Opposite side of the same individual, on which lateral line development has been prevented: melanophores readily colonize the middle of the flank and xanthophores are confined principally to regions in between adjacent ''vertical bars'' of melanophores. Scale bar, 500 μm.

FIG. 4. Fluorescence double exposures of pigment pattern formation in a representative embryo reveal melanophore and xanthophore movements after a subtle melanophore-free region has been established in the path of the midbody lateral line primordium (B37–38). Times after the first appearance of melanophores are: (A) 21, (B) 24, (C) 27, and (D) 30 hr. Anterior is to the right. (A) Two melanophores that retreated ventrally from the midbody lateral line primordium (not shown) are indicated (arrowheads) immediately ventral to the DiI-

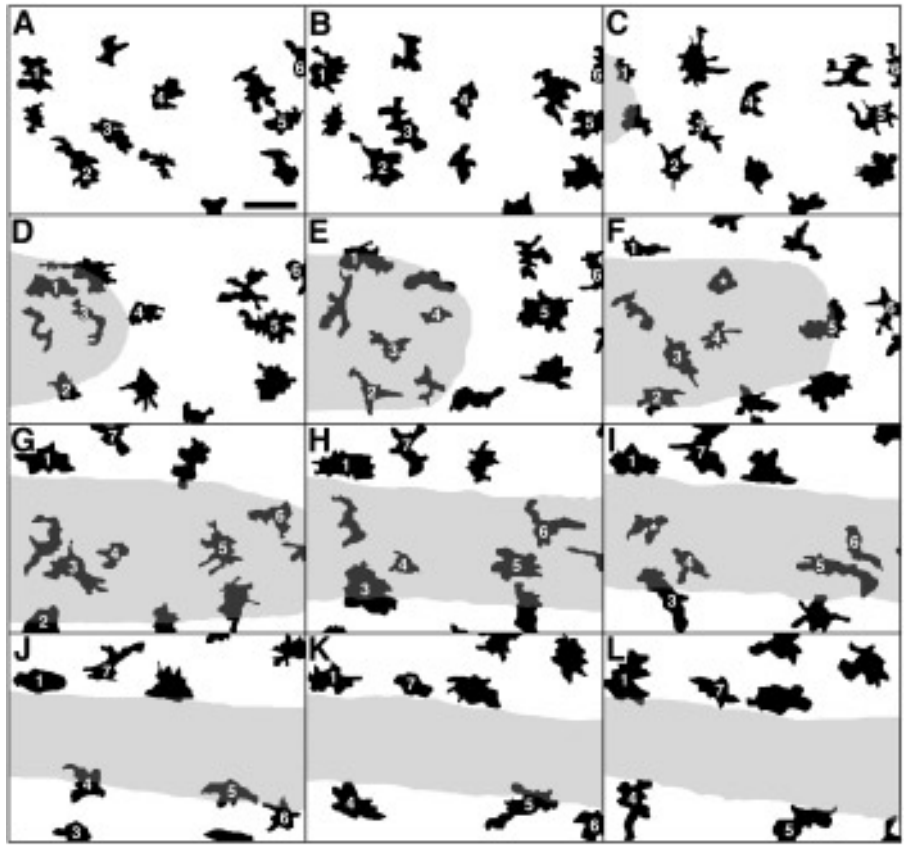

FIG. 3. Time-lapse videomicrography reveals both active and passive melanophore movements during the migration of the midbody lateral line primordium in a representative embryo (B35/36–B37; corresponding to stages shown in Figs. 2C, 2D, 2I, and 2J in Parichy 1996b). Anterior is to the left. Elapsed times in A–L are: 0, 30, 60, 90, 135, 180, 210, 225, 255, 285, 360, and 420 min, respectively. Seven representative melanophores are labeled (cells 1–6 in A–L; cell 7 in G–L) and approximate positions of the Nile blue-stained primordium are indicated in gray. Each of cells 1–6 is overrun by the primordium, with cell 1 emerging dorsally and cells 2–6 emerging ventrally. These movements were accompanied by active extension and retraction of processes, though apparently passive displacements also could be observed (see text). Cell 7 approached the developing lateral line only after the distal tip of the primordium had passed. Some melanophores either were lost from view while subjacent to the primordium (cells indicated with an asterisk in F and I), or migrated out of the field shown. Scale bar, 75 μm.

the myotomes (Figs. 2A and 2C). Prevention of lateral line development allows melanophores to populate the middle of the flank (Fig. 2B; also see Parichy, 1996b). Figure 2D shows that ablation of the lateral lines also perturbs the distribution of xanthophores, which fail to populate the middle of the flank as extensively, and instead retain a pattern specified initially by premigratory aggregates.

---

labeled, midbody lateral line (LL). Dispersing xanthophores align transiently dorsal to the lateral line. (B) Xanthophores soon cross the lateral line (e.g., cells indicated with arrows). (C) As xanthophores approach melanophores already ventral to the lateral line (arrowheads), these melanophores move further toward the yolk mass (D). Small arrow in D indicates one of a few dorsal melanophores in this embryo that eventually cross the lateral line to localize in the middle of the flank. Scale bar, 200 μm (A).

FIG. 5. Younger, donor melanophores and xanthophores in older host embryos. Anterior is to the right in all panels. (A, B) In a host embryo at B38, donor, lightly pigmented melanophores (e.g., arrowhead) and xanthophores (not shown) disperse toward the middle of the flank from a single neural fold grafted to the dorsal epidermis. (C) At later stages (>B43), most melanophores are present dorsally, some are found ventrally, but few occur subjacent (i.e., medial) to the midbody lateral line (arrow). (D) Higher magnification view of the same larva shown in C. A fluorescence double exposure reveals labeled melanophores (e.g., cells indicated with arrowheads) dorsal and ventral to the midbody lateral line, as well as labeled xanthophores (e.g., arrow) subjacent to the lateral line. n, neuromasts. Scale bars: A, B, 200 μm; C, 500 μm; D, 200 μm.

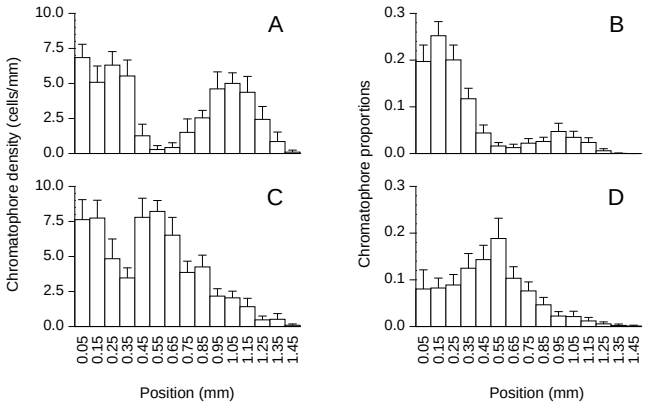

FIG. 6. Quantitation of melanophore and xanthophore distributions in unmanipulated larvae (A, C) and heterochronic chimeras (B, D). Positions (mm) represent distances from the dorsal apex of the myotomes; only midpoint values are provided (for quantitative methods, see Parichy, 1996b). (A and C) In unmanipulated larvae (n = 9 sides of 9 unmanipulated larvae; total cells: 992 melanophores, 1290 xanthophores), chromatophore densities at different positions are normalized according to the length of the region examined. (B and D) In heterochronic chimeras, the numbers of DiI-labeled melanophores and xanthophores varied considerably among larvae, and between sides of individual larvae (melanophores: range = 4–86 melanophores/side, mean = 29.9, SD = 19.71, n = 56 sides of 28 larvae; xanthophores: range = 1–69 xanthophores/side, mean = 22.6, SD = 16.27, n = 53 sides of 27 larvae; total cells: 1668 melanophores, 1197 xanthophores). Consequently the numbers of donor melanophores and xanthophores at different positions are normalized according to the total numbers of labeled cells of each type counted. Unlabeled chromatophores were assumed to be host-derived and are not included. (A) In unmanipulated larvae, melanophore densities are high in dorsal (0.05–0.35 mm) and ventral ($\geq$0.85 mm) regions of the flank, but are low in the vicinity of the midbody lateral line (0.45–0.75 mm). (B) In heterochronic chimeras, the greatest proportions of younger donor melanophores are found in dorsal regions of the flank, and very low proportions are found in the vicinity of the midbody lateral line. (C) Xanthophore densities in unmanipulated larvae display an inverse relationship to melanophores, with low densities dorsal and ventral to the midbody lateral line, but high densities in the middle of the flank. (D) Donor xanthophores in heterochronic chimeras are also abundant in the middle of the flank. Bars, 95% confidence limits.

Early Development of the Melanophore-Free Region

Figure 3 shows typical melanophore movements as recorded in time-lapse videos (n = 8; B35/36–B37) during the early development of the melanophore-free region in a representative embryo. Prior to the appearance of the lateral line primordium, melanophores translocated generally in a dorsal-to-ventral direction, though some were stationary (cells 2 and 1, respectively; Figs. 3A–3C). Mitoses were occasionally observed (4 of 37 melanophores followed). As the primordium entered the field of view, it frequently ''over-ran'' melanophores in its path (cell 1; Figs. 3C–3D). Average velocities at the distal tips of midbody lateral line primordia ranged from 107 to 147 μm/hr across embryos (overall mean = 132 μm/hr, SD = 12.3, n = 7 embryos), and primordia traveled at speeds appreciably greater than melanophores (see Discussion). Primordium migration also was accompanied by rearrangements of surrounding epidermal cells (not shown; see Stone, 1933). Most melanophores overrun by the primordium emerged ventrally or dorsally after 1–5 hr, and such movements were accompanied by active extension and retraction of processes (cells 1 and 2; Figs. 3C–3H). Emerging melanophores sometimes aligned transiently parallel to the primordium (cell 1; Fig. 3F) and often contacted neighboring melanophores, at which time processes were retracted by the translocating cells and extended in different directions (cells 5 and 6; Figs. 3J–3L). Melanophores emerging ventrally moved further from the midpoint of the primordium than melanophores emerging dorsally (least-squares means = 100, 42 μm, SD = 40.7, 40.7, n = 16, 15, respectively; analysis of covariance, $F_{1,28}$ = 15.57, $P < 0.001$). In addition to active movements, melanophores also could be displaced passively short distances when first confronted by the primordium (compare positions of cells 1 and 2; Figs. 3C and 3D). Such displacements could be accompanied by a momentary slowing of primordium advance and compression of the melanophore in its path (cell 5; Figs. 3E and 3F). On rare occasions, melanophores subjacent (i.e., medial) to the primordium were displaced as far as two to three cell diameters caudally, and portions sometimes appeared to be torn repeatedly from such cells (not shown).

After the distal tip of the primordium had passed (B37–38), melanophores in dorsal regions of the flank typically failed to traverse the lateral line (cells 1 and 7; Figs. 3G–3L). Xanthophores were visible in photographic series (n = 17 embryos; Fig. 4; also see Parichy, 1996b) and frequently could be identified in time-lapse videos as active, highly pulsatile cells dispersing in regions of xanthophore bar formation (not shown). Xanthophores often formed transient rows immediately dorsal to the lateral line (Fig. 4A), but then crossed the lateral line to colonize the middle of the flank (Fig. 4B). Concomitantly, adjacent melanophores already ventral to the lateral line could be observed translocating further toward the yolk mass (Figs. 4A–4D). When dorsal melanophores occasionally crossed the lateral line, this event was correlated with a local increase in melanophore number, or the close approach of xanthophores (Fig. 4D). At later stages (>B38), melanophores and xanthophores became increasingly arborized and rearrangements were no longer observed (Parichy, 1996b).

These results indicate that: (i) most melanophores actively translocate from the middle of the flank to establish the melanophore-free region; (ii) some melanophores are displaced passively; and (iii) xanthophores—but not mela-

nophores—cross the lateral line to populate the middle of the flank after primordium migration.

Extracellular vs Autonomous Factors That Maintain the Melanophore-Free Region

After the melanophore-free region is established, most melanophores could fail to repopulate this area because of extracellular factors (e.g., physical barriers or changes in the ECM), or because of cell-autonomous, stage-specific behavioral modifications (e.g., a decrease in locomotory competence, perhaps due to altered expression of cell adhesion molecules as the cells differentiate; see Erickson and Goins, 1995). I investigated these possibilities by examining the behavior of younger chromatophores in older, neural crest-depleted hosts (Fig. 1B), at stages when the melanophore-free region normally would have been formed (e.g., Fig. 4D). If maintenance of the melanophore-free region depends on extracellular factors and does not require autonomous changes in melanophore behavior, then younger melanophores should fail to populate the vicinity of the midbody lateral line. Conversely, if maintenance of the melanophore-free region requires autonomous changes in melanophore behavior, but not extracellular factors, then younger melanophores should populate this area.

Elongated, lightly pigmented donor melanophores (Figs. 5A and 5B) approached the midbody lateral line after the primordium had passed (B37–38). At later stages (>B43), most donor melanophores were found in dorsal regions of the flank and immediately dorsal to the midbody lateral line, and very few were found at the level of the lateral line (Figs. 5C, 5D, and 6B). Nevertheless, a few donor melanophores settled ventral to the lateral line, indicating that observed distributions do not simply reflect poor dispersal, as might be expected if cell densities were insufficient to drive melanophores toward the middle of the myotomes. Donor xanthophores were found dorsally and ventrally, but also in the middle of the flank, and immediately subjacent to the lateral line (Figs. 5D and 6D). These data indicate that: (i) extracellular factors can inhibit melanophores from populating the middle of the flank even after primordium migration; (ii) autonomous, stage-specific changes in melanophore behavior are not absolutely required for maintaining the melanophore-free region (though such changes could still occur during normal development); and (iii) xanthophores are more invasive than melanophores under these conditions. The inhibition of melanophore settling in the middle of the flank appears to depend in part on cues associated with the midbody lateral line, since melanophores were not present immediately subjacent to the lateral line, but were distributed more uniformly in two individuals in which the lateral line primordia failed to migrate.

Physical Relationships of the Lateral Lines with Chromatophores and Surrounding Tissues

Time-lapse videos suggested that steric effects of the lateral line primordium could contribute to establishing the melanophore-free region. Similarly, extracellular factors inferred to maintain the melanophore-free region could reflect steric effects of the lateral lines during later development. Hence, I used SEM and TEM to examine physical relationships of the lateral lines with chromatophores and surrounding tissues.

At B36, a subtle melanophore-free region is evident in the vicinity of the migrating, midbody lateral line primordium (Fig. 3J; also see Figs. 2C and 2I in Parichy, 1996b). In cross section, the primordium can be seen as a distinctive cord of cells within the epidermis at the middle of the flank ($n = 6$; Fig. 7A). Epidermal cells lateral to the primordium are thinner as compared to surrounding regions and a groove is present in the apposing, lateral face of the myotomes. When the epidermis was removed, a distinctive furrow was observed in the myotomes that was deepest and widest near the distal (caudal) tip of the primordium, but shallower in more proximal (rostral) regions ($n = 11$; Fig. 8A). Melanophores and xanthophores occurred at the edge of the furrow, compressed along the walls of the furrow (Fig. 8C), and on the subepidermal basement membrane adjacent to the primordium (Fig. 8D). The lateral lines are responsible for this furrow because embryos in which the lateral line placodes had been ablated failed to display either primordia or furrows in the myotomes ($n = 8$; Fig. 8B). SEM also revealed that the primordium is separated from chromatophores and the myotomes by the subepidermal basement membrane (Fig. 7B). (The basement membrane is defined here to include the subepidermal basal lamina plus associated ECM, as seen with SEM, TEM, or light microscopy.) At the TEM level, the basement membrane bridges a gap between the primordium and epidermis (Figs. 7C and 7D; $n = 3$ embryos), but tended to be thinner and less organized where it covers the medial surface of the primordium (i.e., facing the myotomes), or at the primordium–epidermis junction, as compared to regions further dorsally or ventrally (Figs. 7E–7G). A basement membrane was not apparent at the lateral (i.e., outer) surface of the primordium.

At B40, the definitive early larval pattern is nearly formed and lateral line development is essentially completed (slightly prior to Fig. 2A). In larvae prepared for SEM ($n = 3$), the midbody lateral line nerve could be seen adjacent to the inner epidermis, apposed closely to a subcutaneous artery that runs along the lateral face of the myotomes (Figs. 2A, 7H, and 7I). Identity of the nerve was confirmed by DiI-labeling, and by its absence when the lateral line placodes were ablated (below). After removal of the epidermis, a small furrow was found in the myotomes subjacent to the nerve and dorsal to the subcutaneous artery ($n = 6$), but this furrow was not present in larvae without lateral lines ($n = 4$; not shown). At the TEM level, the subepidermal basement membrane at B40 (Fig. 7J; $n = 3$ larvae) was thicker than at B36.

These findings are consistent with the hypotheses that: (i) the primordium has steric effects on surrounding tissues, with correlated effects on melanophores; and (ii)

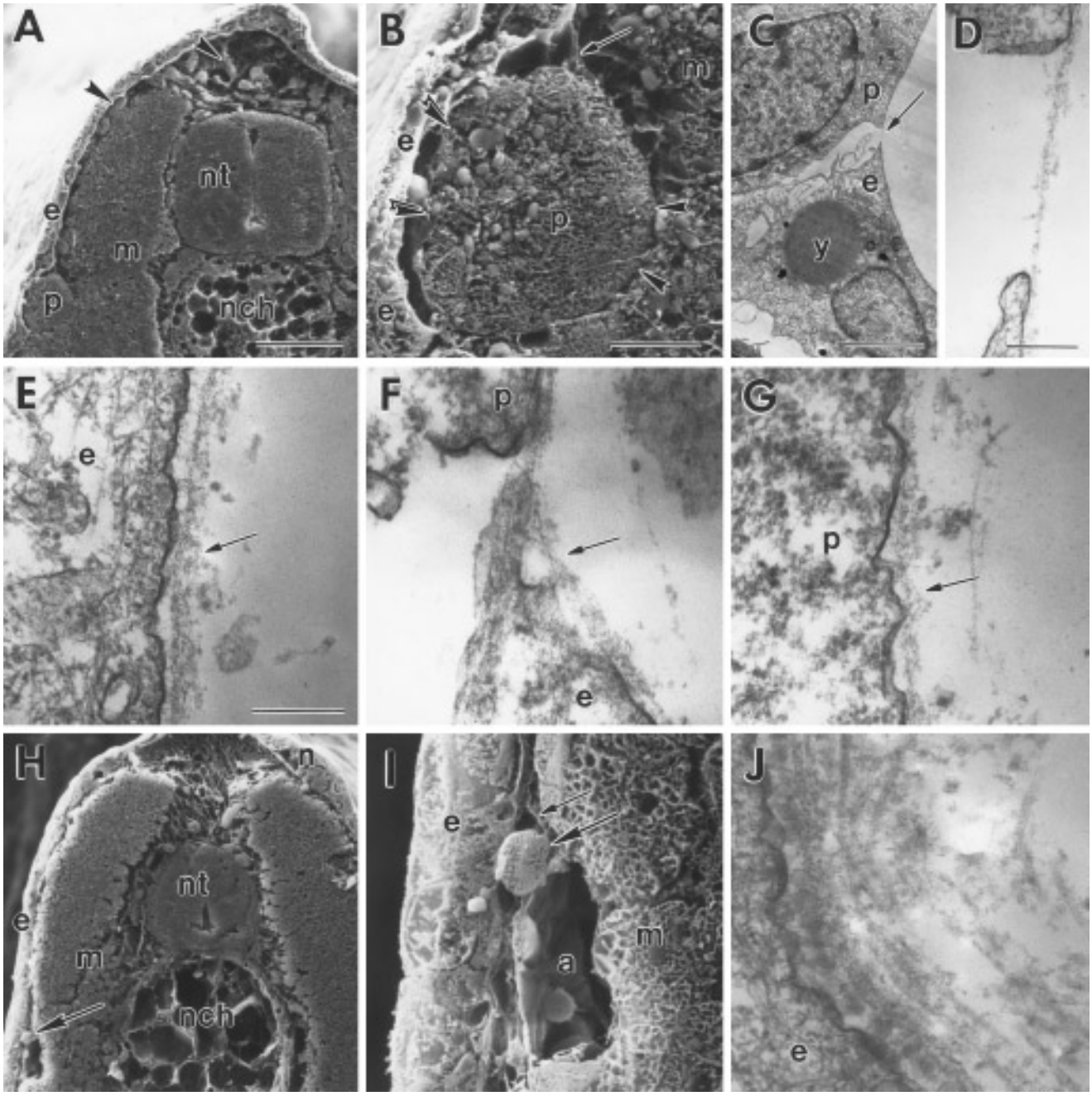

FIG. 7. Physical relationships of the lateral lines with surrounding tissues revealed by scanning and transmission electron microscopy. (A–G) Stage B36. (H–J) Stage B40. (A) At B36, chromatophores and neural crest cells (arrowheads) are found dorsal to the neural tube (nt) and in the space between the epidermis (e) and myotomes (m). The midbody lateral line primordium (p) is found within the epidermis and has migrated approximately half the length of the trunk. (B) A higher magnification view of the primordium in A, showing relationships with surrounding epidermal cells, as well as the subepidermal basement membrane (arrow) extending from the epidermis to cover the primordium. Single arrowheads indicate the medial (inner) surface of the primordium and double arrowheads indicate the lateral (outer) surface of the primordium. (C) Low-magnification TEM micrograph at the junction between a cell of the lateral line primordium (p) and an adjacent, ventral epidermal cell (e), illustrating the subepidermal basement membrane (arrow) spanning the gap between the two cells. A yolk platelet (y) is indicated and small, black organelles are maternal melanosomes. (D) Detail of the region indicated with an arrow in C. (E–G) High-magnification views of the subepidermal basement membrane. (E) A continuous and organized basement membrane (arrow) is present ventral to the migrating primordium. (F) At the junction between the primordium and epidermis, the basement membrane is disorganized. (G) At the medial-most portion of the lateral line primordium (corresponding to single arrowheads in B), the basement membrane is patchy and flocculent. (H) At B40, the lateral line nerve (arrow) is found between the epidermis and myotomes, and a dorsal

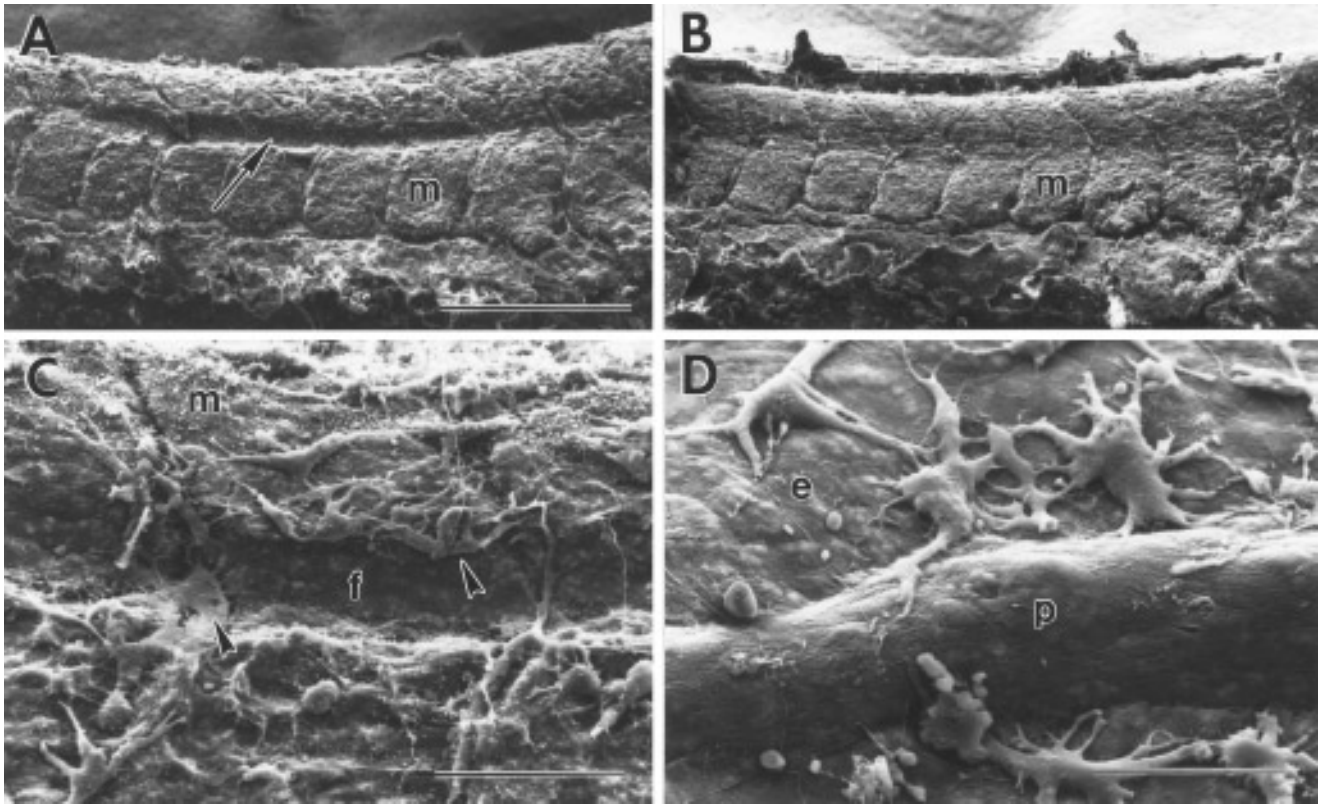

FIG. 8. Physical relationships between the lateral line primordium, myotomes, and chromatophores. Anterior is to the right in all panels. (A) In an unmanipulated embryo (B36), a deep furrow (arrow) is found in the myotomes (m) immediately subjacent to the migrating lateral line primordium. (B) When lateral line development is prevented, however, no furrow is found in the myotomes at the same stage of development. (C) A higher magnification view in a different embryo of the furrow (f) created in the myotomes by the lateral line primordium, with chromatophores at the dorsal edge of the furrow and medially within the furrow (arrowheads). (D) Melanophores on the subepidermal basement membrane near the distal tip of the primordium. Scale bars: (A,B) 400 μm; (C) 100 μm; (D) 50 μm.

the lateral line nerve acts as a physical obstacle that inhibits the migration or settling of melanophores in the middle of the flank.

Distributions of Extracellular Matrix Components

Accumulating evidence indicates that the composition of the ECM influences the morphogenesis of neural crest cells and chromatophores (reviewed in Erickson, 1993; Erickson and Perris, 1993). For example, chondroitin sulfate proteoglycans and molecules that bind the lectin peanut agglutinin (PNA) correlate with barriers to the migration of these cells, whereas fibronectin and laminin occur along migratory pathways (e.g., Tucker, 1986; Epperlein *et al.*, 1988; Perris *et al.*, 1990; Oakley *et al.*, 1994; Spence and Poole, 1994; Tosney *et al.*, 1994; Krull *et al.*, 1995; Landolt *et al.*, 1995). Indeed, studies of other salamanders have suggested that melanophore-free regions are established because chromatophores respond to localized cues in the ECM: tenascin and chondroitin sulfate proteoglycans are believed to have ''anti-adhesive'' effects, excluding melanophores from the middle of the flank (Epperlein and Löfberg, 1990, 1993), whereas fibronectin is hypothesized to act as an adhesive substratum, trapping melanophores at sites of stripe formation (Tucker and Erickson, 1986a,b). Given these previous findings, the demonstration that the lateral lines are responsible for the melanophore-free region in *A. t. tigri-*

lateral line neuromast (n) is visible on the contralateral flank. (I) Detail of the larva shown in H, showing the midbody lateral line nerve (large arrow) covered by basement membrane (small arrow) and apposed closely to a subcutaneous artery (a), running along the lateral face of the myotomes (m). (J) The subepidermal basement membrane has thickened considerably by B40. The representative section is taken from the vicinity of the lateral line nerve, corresponding to the dorsoventral position in G. Scale bars: (A, H) 100 μm; (B, I) 20 μm; (C) 400 nm; (D) 200 nm; (E–G, J) 200 nm: nch, notochord.

TABLE 1
Sample Sizes for Analyses of Extracellular Matrices

ECM component	Embryos examined[a]				Total
	B32–33	B35–36	B38–39	B40–42	
Tenascin	8	13	8	11	40
Chondroitin sulfate proteoglycans	4	9	3	10	26
Laminin	9	10	4	9	32
Fibronectin	7	10	3	11	31
PNA-binding activity	8	10[b]	3	9	30

[a] B35–36, B38–39, and B40–42 embryos received unilateral lateral line ablations.
[b] Includes 2 stage B37 embryos.

num suggests that effects on melanophores could be mediated by lateral line-dependent changes in the matrix (e.g., appearance of anti-adhesive molecules or disappearance of adhesive molecules). To investigate this possibility, I examined the distribution of ''candidate'' patterning molecules (PNA-binding activity, tenascin, chondroitin sulfate proteoglycans, fibronectin, laminin) during neural crest cell migration (B32/33; Olsson and Löfberg, 1992) and pigment pattern formation (B35–42), in the presence and absence of lateral lines (Fig. 1A; Table 1).

None of the ECM components examined were localized exclusively within or outside of the melanophore-free region (Figs. 9 and 10). Nevertheless, comparisons of lateral line-intact and -ablated sides revealed three effects of lateral line development. (1) During establishment of the melanophore-free region (B35/36), discontinuities in the subepidermal basement membrane sometimes could be detected at the junction between the primordium and epidermis, or along the medial aspect of the primordium (e.g., PNA-binding activity, Fig. 9D), consistent with TEM observations. Similarly in the wake of the primordium (B37), breaches in the basement membrane were observed in the vicinity of prospective neuromasts and the lateral line nerve, which passes from the apical to the basal surface of this membrane (Figs. 9H, 9G, 9F, 9E, and 10O; also see Sato, 1976; Winklbauer, 1989). More subtle discontinuities also were associated with the much smaller dorsal lateral line (e.g., Fig. 9C), which generates a small and transient melanophore-free region (Parichy, 1996b). In contrast, gaps in basement membrane staining were not present on lateral line-ablated sides (not shown). (2) Although the subepidermal basement membrane was continuous after primordium migration (B38–42), the lateral line nerve was covered by a layer of basement membrane extending from beneath the epidermis (Figs. 10C, 10G, 10K, and 7I). Sides without lateral lines did not exhibit such ''projections'' of basement membrane (Fig. 10H). (3) Tenascin staining was slightly enhanced in the vicinity of the lateral line during B38–42, as compared to equivalent regions on lateral line-ablated sides (Figs. 10G and 10H).

In addition to lateral line effects, dramatic lateral line-*independent* increases in staining were observed for PNA-binding activity (Figs. 9A–9C), tenascin (Figs. 10A–10F), and laminin (Figs. 10I–10K) throughout the embryo by terminal stages of pigment pattern formation (B38–42). This elaboration of the matrix coincided with a rapid expansion of the flank that occurs principally after the midbody lateral line primordium has passed (Fig. 11).

These results indicate that: (i) establishment of the melanophore-free region probably does not depend on specific, lateral line-dependent regulation of the abundance of these ECM components; (ii) lateral line-dependent, structural perturbations of the subepidermal basement membrane correlate with the initial evacuation and early exclusion of melanophores from the middle of the flank; and (iii) enhanced, lateral line-dependent deposition of tenascin and a lateral line-independent elaboration of the matrix coincide with increasingly stable melanophore positions during terminal stages of pigment pattern formation (Parichy, 1996b).

DISCUSSION

The factors underlying a distinctive melanophore-free region in *A. t. tigrinum* can be conceptualized as falling into two classes: those that cause initially widely distributed melanophores to be depleted from the middle of the flank, thus establishing the melanophore-free region; and those that prevent melanophores from repopulating this area, thereby maintaining the melanophore-free region during later development. This study demonstrates that: (i) most melanophores respond to the lateral line primordium by evacuating the middle of the flank; and (ii) extracellular factors can prevent melanophores from colonizing this region after primordium migration. Additionally, these data are consistent with the hypothesis that development of the melanophore-free region depends on multiple factors, including steric effects, interactions between melanophores and xanthophores, and changes in the ECM.

Establishment of the Melanophore-Free Region

The melanophore-free region is established (B35/36–37) because most melanophores actively retreat short distances

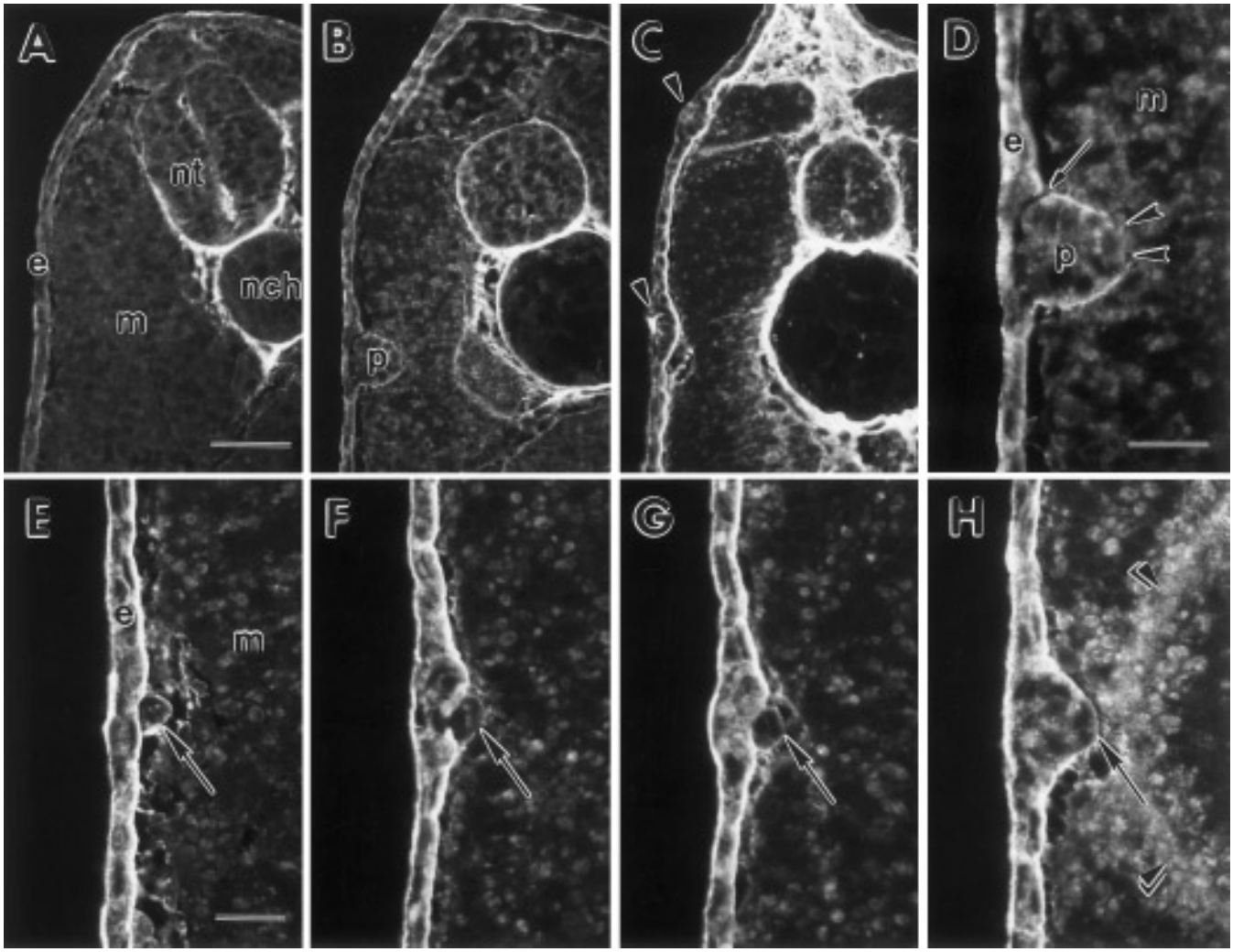

FIG. 9. PNA-binding activity. Representative sections in A–C were stained, photographed, and printed identically. (A) Only low levels of PNA-binding activity are observed between the epidermis (e) and myotomes (m) during neural crest cell migration (B32/33). (B) During the migration of the midbody lateral line primordium (B35/36), PNA-binding activity is present subepidermally and also covers the primordium (p; higher magnification view in D). (C) By terminal stages of pigment pattern formation (B40/41), PNA-binding activity has increased dramatically in the subepidermal basement membrane and interstitial matrices throughout the embryo. Arrowheads indicate neuromasts of the dorsal and midbody lateral lines. (D) Although the primordium is generally covered by PNA-binding basement membrane, gaps could be detected along the medial surface of the primordium (between arrowheads) and at the junction between the primordium and adjacent epidermis (arrow). (E–H) Anterior (E) to posterior (H) sections of a single B37 embryo showing breaches in the subepidermal basement membrane as the lateral line nerve (arrow) passes from the apical to the basal surface of this membrane. Anteriorly (E), the nerve is present between the epidermis and a developing artery (e.g., Fig. 7I), but further posteriorly (H) the nerve contacts the lateral line primordium (double arrowheads indicate PNA-binding activity within a myoseptum). nch, notochord; nt, neural tube. Scale bars: (A–C) 100 μm; (D) 40 μm; (E–H) 30 μm.

from the migrating, midbody lateral line primordium. In turn, several lines of evidence suggest that this event could be mediated by steric effects of the primordium on surrounding tissues and melanophores. For example, the primordium migrates within the epidermis, yet the subepidermal basement membrane is unusually patchy and flocculent where it covers the primordium, or spans the junction between the primordium and epidermis. Moreover, the primordium is responsible for a deep furrow in the subjacent myotomes, and chromatophores lining the walls of this furrow can exhibit compressed morphologies. Finally, melanophores retreat only after contacting the basement membrane-covered primordium, and initial encounters between melanophores and the primordium could be accompanied by a slowing of primordium advance, as well as compression, passive displacement, or even fragmentation of mela-

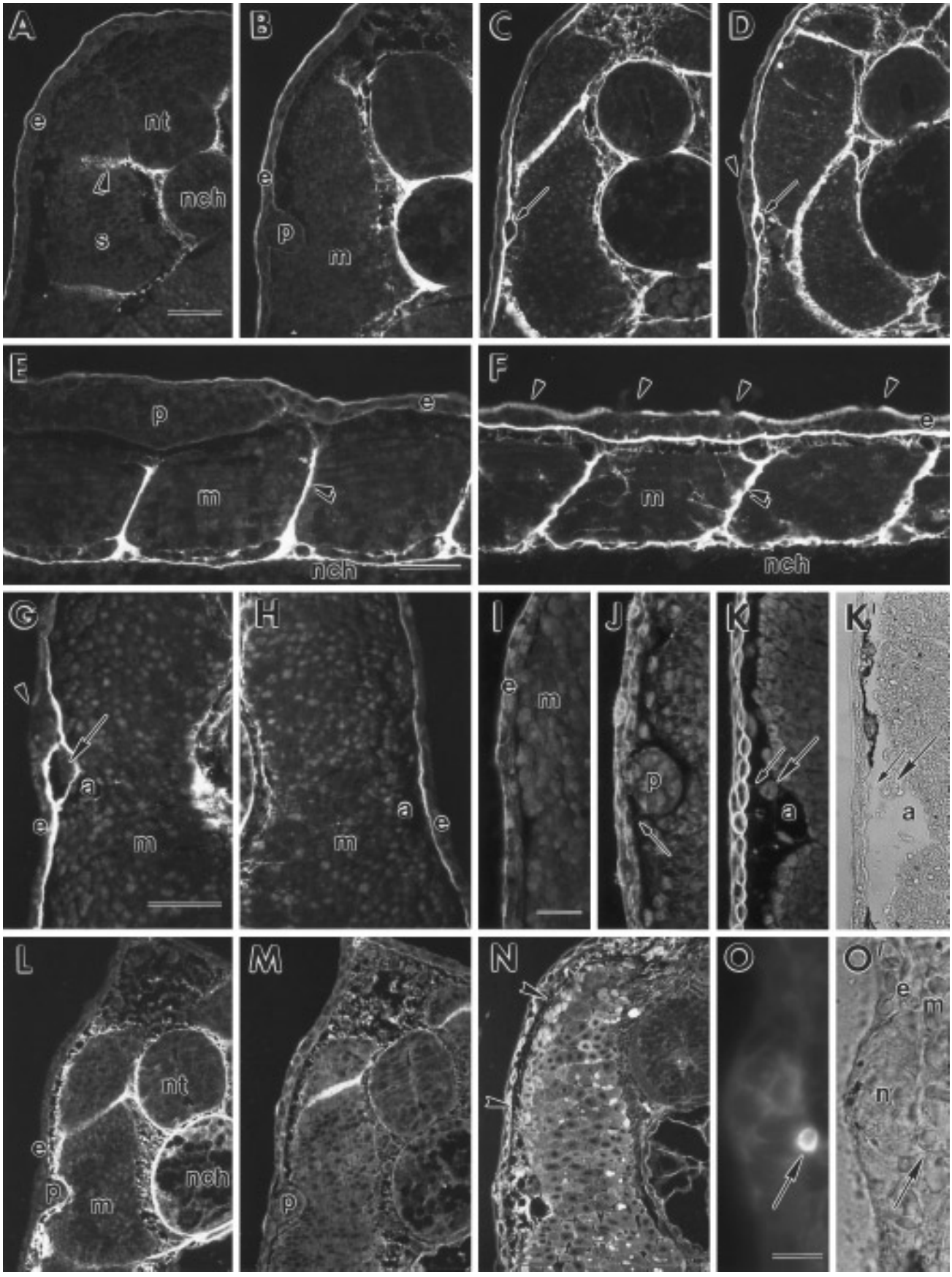
A
e
nt
nch
s
B
e
p
m
C
D
E
p
e
m
nch
F
e
m
nch
G
a
e
m
H
a
e
m
I
e
m
J
p
K
a
K'
a
L
nt
e
nch
p
m
M
p
N
O
O'
e
m
n

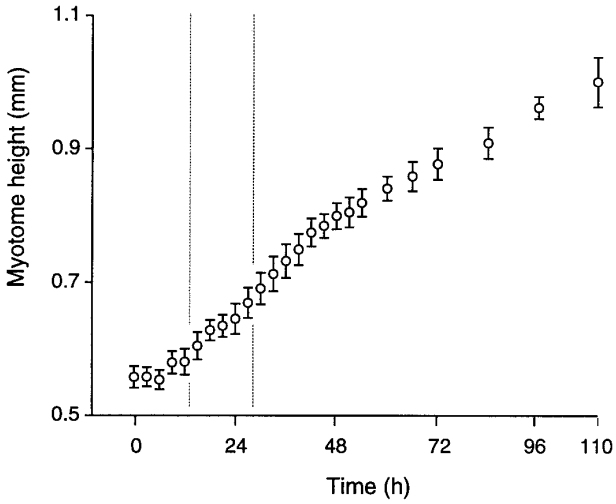

FIG. 11. Dorsal–ventral extension of the myotomes occurs principally after migration of the midbody lateral line primordium and coincides with an elaboration of the ECM (0 hr = B35, 110 hr = B42; n = 17 embryos). Each point represents the mean dorsal–ventral height of the myotomes at a fixed position in the middle of the trunk. Vertical dotted lines indicate the range of times at which the distal tip of the midbody lateral line primordium had passed the region measured. Bars, 95% confidence limits.

nophores. These findings imply that the primordium exerts powerful forces against surrounding tissues and melanophores, and probably also shears or distends the subepidermal basement membrane as it migrates. The large size and high speed of the primordium are consistent with these inferences: the primordium is several cells thick and travels as fast as 107–147 μm/hr. For comparison, the average velocity of *A. mexicanum* melanophores is only 42 μm/hr (Keller and Spieth, 1984) and the maximal reported velocity for *T. torosa* melanophores is 18 μm/hr (Tucker and Erickson, 1986a). The primordium also might perturb the basement membrane by exerting tractional forces (e.g., Harris *et al.*, 1981; Tucker *et al.*, 1985), though the mechanisms underlying primordium motility are not known. Interestingly, lateral lines on the head are not associated with distinctive melanophore-free regions and arise not from freely migrating primordia, but from elongating sensory ridges (Winklbauer, 1989; Northcutt *et al.*, 1994; Parichy, 1996a).

How could steric effects of the midbody lateral line primordium influence melanophores? If disruption of the subepidermal basement membrane generates a relatively weak and unstable substratum for melanophores that interact with this matrix (also see Epperlein, 1982; Epperlein and Claviez, 1982; Keller *et al.*, 1982; Löfberg *et al.*, 1985; Tucker *et al.*, 1985; Tucker and Erickson, 1984, 1986a), even random movements should bring these cells into contact with more favorable regions, dorsal or ventral to the primordium. As melanophores begin to emerge from subjacent to the primordium, compression and spatial constraints also could contribute to biasing further movements away from this region. Additionally, time-lapse videos revealed that although many of the melanophores that evacuate the middle of the flank are already translocating when confronted by the primordium, other melanophores initially are stationary. Thus, the primordium also can stimulate the motility of melanophores, perhaps by disrupting the subepidermal basement membrane or imparting mechanical stresses to the melanophores themselves (Tickle and Trinkaus,

FIG. 10. Immunohistochemistry for candidate patterning molecules of the ECM, and DiI-labeling of the lateral line nerve. (A–H) Tenascin. (I–K) Laminin. (L) Chondroitin sulfate. (M, N) Fibronectin. (O) DiI-labeling. Sets of images for each matrix component (A–D, E–F, G–H, I–K, M–N) were stained, photographed, and printed identically. (A–H) Tenascin staining was qualitatively similar with a polyclonal antiserum (A–F) and mAb M1 (G–H). (A) During neural crest cell migration (B32/33), anti-tenascin immunoreactivity is not observed between the epidermis (e) and somites (s), but is found around the neural tube (nt) and notochord (nch), and in the intersomitic furrows (double arrowhead). Outer epidermal staining is nonspecific. (B) During primordium migration (B35/36), tenascin staining is present in the subepidermal basement membrane and covering the lateral line primordium (p). m, myotome. (C, D) After primordium migration (B38/39, B40/41, respectively), tenascin staining has increased dramatically in the subepidermal basement membrane and interstitial matrix between the epidermis and myotomes, and an anti-tenascin-immunoreactive basement membrane covers the lateral line nerve (arrow; a midbody lateral line neuromast is indicated with an arrowhead in D). (E, F) Frontal sections showing tenascin staining beneath the epidermis at the level of the midbody lateral line at B35/36 (E) and B40/41 (F). Anterior is to the left and double arrowheads indicate staining in the myosepta. The lateral line primordium (p) can be seen migrating within the epidermis in E, and four lateral line neuromasts (arrowheads) are visible in F. (G, H) Tenascin staining on lateral line-intact and -ablated sides from the same section of a B38/39 larva. (G) Pronounced tenascin staining is observed subepidermally and covering the lateral line nerve (arrow) which is apposed to a subcutaneous artery (a); the arrowhead indicates a neuromast. (H) Staining is less intense in the absence of lateral line development. (I–K) Anti-laminin-immunoreactivity is weak initially (I, B32/33) but has increased in the epidermis (and surrounding myocytes) during primordium migration (J, B35/36) and is particularly strong subepidermally during terminal stages of pigment pattern formation (K, B40/41). (K′) A brightfield image corresponding to K, showing melanophores on the subepidermal basement membrane. Small arrows in J–K′ indicate basement membrane projecting from the epidermis to cover either the primordium or the lateral line nerve, and large arrows in K and K′ indicate the lateral line nerve adjacent to an artery (a). (L) Chondroitin sulfate is widely distributed at all stages examined and patterns were qualitatively similar using mAbs ΔDi-6S and CS-56 (shown here at B35/36). (M, N) Staining for fibronectin is widely distributed at all stages (M, B35/36; N, B40/41). Arrowheads in N delineate the position of melanophores, quenching fluorescence in this region. (O, O′) Corresponding fluorescent and brightfield images showing DiI-labeling of the midbody lateral line nerve (arrow), subjacent to a DiI-labeled neuromast (n). Scale bars: (A–D, L–N) 100 μm; (E, F) 100 μm; (G, H) 80 μm; (I–K′) 50 μm, (O, O′) 20 μm.

1976). Although cell–cell interactions leading to contact inhibition of movement (Abercrombie, 1970) and contact stimulated migration (Thomas and Yamada, 1992) probably contribute to the early dispersal of neural crest cells and melanophores (Rovasio *et al.*, 1983; Erickson, 1985; Tucker and Erickson, 1986a), neither of these phenomena adequately explain the present observations, since the cells of the primordium are separated from melanophores by the subepidermal basement membrane.

Horizontal stripes in other salamanders are hypothesized to form because chromatophores respond to cues in the ECM (Tucker and Erickson, 1986a,b; Epperlein and Löfberg, 1990, 1993). In this study, comparison of lateral line-intact and -ablated sides during primordium migration did not reveal differences in staining for ''candidate'' patterning molecules [PNA-binding molecules, tenascin, chondroitin sulfate proteoglycans, fibronectin, laminin; or keratan sulfate proteoglycans and hyaluronan (Tucker and Erickson, 1984, 1986b; Olsson *et al.*, 1996), unpublished data; reviewed in Erickson, 1993; Erickson and Perris, 1993]. This suggests that the lateral lines do not specifically alter the abundance of these matrix components to establish the melanophore-free region. Since lateral line-dependent melanophore-free regions are inferred to be ancestral for ambystomatids and salamandrids (Parichy, 1996b), an intriguing hypothesis is that putative ECM cues for establishing stripes in other taxa represent an evolutionary innovation in patterning mechanisms. Nevertheless, the present results do not rule out roles for additional lateral line-dependent factors that might contribute to excluding melanophores from the middle of the flank (e.g., different ECM components or chemorepellants; Twitty and Niu, 1948; Colamarino and Tessier-Lavigne, 1995). These possibilities are currently being investigated.

Maintenance of the Melanophore-Free Region

After melanophores retreat from the primordium, these cells might be expected to recolonize in its wake because of random motility, contact inhibition of movement (Rovasio *et al.*, 1983; Erickson, 1985; Tucker and Erickson, 1986a), continued proliferation, and interactions with dispersing xanthophores. Nevertheless, the melanophore-free region persists and becomes increasingly distinctive (≥B37). One hypothesis to explain the maintenance of this pattern element is that melanophores undergo autonomous, age- or differentiation-specific changes that prevent them from repopulating the middle of the flank (e.g., a loss of locomotory competence, perhaps due to expression of different adhesion molecules; see Delannet *et al.*, 1994; Hara *et al.*, 1994; Qian *et al.*, 1994; Tang *et al.*, 1994; Beauvais *et al.*, 1995; Erickson and Goins, 1995). In heterochronic chimeras, however, most younger, lightly pigmented and elongated donor melanophores (dispersing after primordium migration) failed to settle immediately subjacent to the lateral line or further ventrally over the myotomes. These data suggest that during normal development, autonomous, stage-specific changes in melanophore behavior are not absolutely required for maintaining the melanophore-free region and imply instead that extracellular factors can inhibit melanophores from repopulating the middle of the flank.

Factors associated with the midbody lateral line nerve are likely candidates for inhibiting dorsal melanophores from migrating further ventrally once the melanophore-free region has been established. Shortly after the distal tip of the primordium passes (B37), the position of the lateral line nerve correlates with breaches in the subepidermal basement membrane. Subsequently, however, the nerve is found medial to the epidermis, apposed to an artery that develops along the lateral face of the myotomes, and the nerve is covered by a layer of basement membrane that is contiguous with the subepidermal basement membrane. These observations suggest that melanophores could be inhibited initially from recolonizing in the wake of the primordium if disruptions of the subepidermal basement membrane present a relatively nonpermissive substratum as compared to adjacent, intact basement membrane. Melanophore movements also could be retarded if the nerve acts as an obstacle because of space constraints (e.g., Bard *et al.*, 1975; Löfberg and Ahlfors, 1978; Löfberg *et al.*, 1980; Thiery *et al.*, 1982; Ranscht and Bronner-Fraser, 1991), or because of its curvature (Dunn and Heath, 1976; Dunn, 1982), or if the basement membrane that covers the nerve at later stages is a relatively pliable and unstable substratum (Tucker and Erickson, 1984; Tucker *et al.*, 1985). Physical features of the extracellular environment are not expected to act as absolute barriers, but could be especially effective when combined with other factors that inhibit melanophore motility (below; see Newgreen, 1989).

The data presented here also implicate interactions between melanophores and xanthophores in maintaining the melanophore-free region. Dispersing xanthophores often form transient rows dorsal to the lateral line nerve, as if delayed temporarily in their migration. Unlike melanophores, however, xanthophores cross the lateral line to colonize the middle of the flank, both during normal development (also see Parichy, 1996b) and in heterochronic chimeras. A variety of factors could make xanthophores more invasive than melanophores: for example, xanthophores could be smaller or more deformable (Tickle and Trinkaus, 1973; Erickson, 1980), or could exhibit enhanced locomotory capability (Gail and Boone, 1971; Paddock and Dunn, 1986; Tucker and Erickson, 1986b; also see Erickson and Goins, 1995), perhaps resulting from differences in the expression of proteases (Seftor *et al.*, 1992; Stetler-Stevenson *et al.*, 1993; Duong and Erickson, 1995) or molecules regulating cell–matrix adhesion (Faassen *et al.*, 1992; Thomas *et al.*, 1992; Beauvais *et al.*, 1995). The ability of xanthophores to rapidly occupy ''chromatophore-free space'' in the wake of the primordium (≥B37) almost certainly confers upon these cells a role in inhibiting melanophores from returning to this area (e.g., by contact inhibition of movement) and probably also causes melanophores to recede further from the lateral line nerve. Consistent with these ideas, melanophores emerging ventrally from subjacent to the primordium (away from dispersing xanthophores) move

greater distances than melanophores emerging dorsally, and melanophores already ventral to the lateral line translocate further toward the yolk mass after being approached by xanthophores. Thus, melanophore–xanthophore interactions that translate a prepattern of xanthophore aggregates into a vertical barring pattern (Lehman, 1957; Epperlein and Löfberg, 1990; Olsson and Löfberg, 1992) probably also contribute to translating a prepattern established by melanophore–primordium interactions into a distinctive melanophore-free region. This leads to the prediction that in taxa displaying both vertical bars and melanophore-free regions, evolutionary changes in the complements of melanophores and xanthophores should yield correlated responses in both pattern elements (e.g., compare *A. t. tigrinum* with *A. barbouri* in Parichy, 1996b).

After a melanophore-free region is established (≥B37), melanophores are increasingly arborized and during terminal stages of pigment pattern formation (≥B38), rearrangements are no longer observed (see Parichy, 1996b). Examination of ''candidate'' patterning molecules (B38–42) suggests that changes in the ECM could contribute to this cessation of melanophore motility. Staining for tenascin was enhanced in the vicinity of the midbody lateral line as compared to lateral line-ablated sides, perhaps reflecting a difference between ''wounded'' and unperturbed matrices, or differences in proliferative activity within the epidermis (Mackie *et al.*, 1988; Smith *et al.*, 1988). In addition, lateral line-*independent* increases in staining were observed for tenascin, laminin, and PNA-binding molecules subepidermally throughout the embryo, and a marked thickening of the basement membrane was evident at the TEM level. *In vitro*, tenascin is a relatively nonadhesive substratum for a variety of cell types (Chiquet-Ehrismann *et al.*, 1988; Epperlein *et al.*, 1988; Wehrle-Haller and Chiquet, 1993) including *A. t. tigrinum* melanophores (Parichy, unpublished data), laminin promotes melanocyte dendricity (Zambruno *et al.*, 1993; Hara *et al.*, 1994), and high concentrations of tenascin, laminin, and collagen each can inhibit neural crest cell motility (Tucker and Erickson, 1984; Perris and Johansson, 1987; Halfter *et al.*, 1989). *In vivo*, PNA-binding molecules correlate with barriers to neural crest cell migration (Oakley *et al.*, 1994; Krull *et al.*, 1995; also see Davies *et al.*, 1990), and increased abundance of basement membrane components correlates with positional stability for other cell types derived from the neural crest (see Erickson and Perris, 1993). These observations suggest that during terminal stages of pigment pattern formation, enhanced tenascin deposition in the vicinity of the lateral line could inhibit melanophores from repopulating this area, and a general elaboration of the matrix could contribute to maintaining the melanophore-free region by retarding the motility of melanophores throughout the embryo. Finally, despite the apparent stability of melanophore positions, the melanophore-free region nevertheless becomes increasingly distinctive at these later stages (e.g., dorsal melanophores initially adjacent to the lateral line nerve are found increasingly distant from this structure; see Figs. 2E, 2F, 2K, and 2L in Parichy, 1996b). This change in the pigment pattern coincides with a rapid increase in the height of the flank, suggesting that if melanophores are ''trapped'' by an increasingly elaborate matrix, overall shape changes could enhance the distinctiveness of the melanophore-free region by separating relatively stable, dorsal and ventral concentrations of melanophores.

A Primitive Mechanism for Stripe Formation

The data presented here prompt a *working hypothesis* for the formation of the melanophore-free region in *A. t. tigrinum:* (1) Melanophores initially disperse widely over the somites. (2) As the midbody lateral line primordium migrates on the apical side of the subepidermal basement membrane, a subtle melanophore-free region is established because melanophores retreat from the middle of the flank in response to steric effects of the primordium on surrounding tissues and the subepidermal basement membrane. (3) The melanophore-free region is maintained initially because of lateral line-dependent discontinuities in the subepidermal basement membrane, and because the lateral line nerve acts as a physical obstacle to melanophore migration and localization. (4) Meanwhile, more invasive xanthophores colonize the vicinity of the midbody lateral line, and thereby contribute to excluding melanophores from the middle of the flank. (5) During terminal stages of pigment pattern formation, melanophore positions are stabilized by an increasingly elaborate subepidermal matrix. Since lateral line-dependent melanophore-free regions are inferred to be primitive for ambystomatids and salamandrids, this hypothesis provides a context for interpreting the phylogenetic diversification of pattern-forming mechanisms (see Parichy, 1996b). Finally, the results of this study raise the possibility that lateral line effects on pigment patterns also might be present in more distantly related amphibians and fishes, if the lateral lines in these taxa develop as in *A. t. tigrinum*.

ACKNOWLEDGMENTS

Thanks to P. B. Armstrong, C. A. Erickson, D. W. Raible, M. V. Reedy, H. B. Shaffer, R. P. Tucker, S. R. Voss, and two anonymous reviewers for insightful comments on various drafts of the manuscript, as well as R. Harris for advice on electron microscopy. This research has been supported by NSF Dissertation Improvement Grant IBN-9423116, a Jastro-Shields Graduate Research Scholarship, a University of California Davis Graduate Research Award, a Sigma Xi Grant-in-Aid of Research, and NIH grants DE05630 and GM53258 to C. A. Erickson. I have been supported by an NSF Predoctoral Fellowship as well as graduate fellowships from the Center for Population Biology (University of California Davis) and the Northern California Regional Association of Phi Beta Kappa.

REFERENCES

Abercrombie, M. (1970). Contact inhibition in tissue culture. *In Vitro* 6, 128–142.

Asashima, M., Malacinski, G. M., and Smith, S. C. (1989). Surgical manipulation of embryos. *In* ''Developmental Biology of the Axolotl'' (J. B. Armstrong and G. M. Malacinski, Eds.), pp. 253–263. Oxford Univ. Press, New York.

Avnur, Z., and Geiger, B. (1984). Immunocytochemical localization of native chondroitin-sulfate in tissues and cultured cells using specific monoclonal antibody. *Cell* 38, 811–822.

Bard, J. B. L., Hay, E. D., and Meller, S. M. (1975). Formation of the endothelium of the avian cornea: A study of cell movement *in vivo*. *Dev. Biol.* 42, 334–361.

Beauvais, A., Erickson, C. A., Goins, T., Craig, S. E., Humphries, M. J., Thiery, J. P., and Dufour, S. (1995). Changes in the fibronectin-specific integrin expression pattern modify the migratory behavior of sarcoma S180 cells in vitro and in the embryonic environment. *J. Cell Biol.* 128, 699–713.

Bordzilovskaya, N. P., Dettlaff, T. A., Duhon, S. T., and Malacinski, G. M. (1989). Developmental-stage series of axolotl embryos. *In* ''Developmental Biology of the Axolotl'' (J. B. Armstrong and G. M. Malacinski, Eds.), pp. 201–219. Oxford Univ. Press, New York.

Boucaut, J.-C., and Darribère, T. (1983). Fibronectin in early amphibian embryos: Migrating mesodermal cells contact fibronectin established prior to gastrulation. *Cell Tissue Res.* 234, 135–145.

Boucaut, J.-C., Darribère, T., Boulekbache, H., and Thiery, J. P. (1984). Prevention of gastrulation but not neurulation by antibodies to fibronectin in amphibian embryos. *Nature* 307, 364–367.

Bronner-Fraser, M. (1994). Neural crest cell formation and migration in the developing embryo. *FASEB J.* 8, 699–706.

Bronner-Fraser, M., and Fraser, S. (1989). Developmental potential of avian trunk neural crest cells in situ. *Neuron* 3, 755–766.

Caubit, X., Riou, J.-F., Coulon, J., Arsanto, J.-P., Benraiss, A., Boucaut, J.-C., and Thouveny, Y. (1994). Tenascin expression in developing, adult and regenerating caudal spinal cord in the urodele amphibians. *Int. J. Dev. Biol.* 38, 661–672.

Chiquet, M., and Fambrough, D. M. (1984). Chick myotendinous antigen. I. A monoclonal antibody as a marker for tendon and muscle morphogenesis. *J. Cell Biol.* 98, 1926–1936.

Chiquet-Ehrismann, R., Kalla, P., Pearson, C. A., Beck, K., and Chiquet, M. (1988). Tenascin interferes with fibronectin action. *Cell* 53, 383–390.

Colamarino, S. A., and Tessier-Lavigne, M. (1995). The axonal chemoattractant netrin-1 is also a chemorepellent for trochlear motor axons. *Cell* 81, 621–629.

Collazo, A., Bronner-Fraser, M., and Fraser, S. E. (1993). Vital dye labeling of *Xenopus laevis* trunk neural crest reveals multipotency and novel pathways of migration. *Development* 118, 363–376.

Collazo, A., Fraser, S. E., and Mabee, P. M. (1994). A dual embryonic origin for vertebrate mechanoreceptors. *Science* 264, 426–430.

Couchman, J. R., Caterson, B., Christner, J. E., and Baker, J. R. (1984). Mapping by monoclonal antibody detection of glycosaminoglycans in connective tissues. *Nature* 307, 650–652.

Couly, G. F., Coltey, P. M., and Le Douarin, N. M. (1993). The triple origin of skull in higher vertebrates: A study in quail–chick chimeras. *Development* 117, 409–429.

Davies, J. A., Cook, G. M. W., Stern, C. D., and Keynes, R. J. (1990). Isolation from chick somites of a glycoprotein fraction that causes collapse of dorsal root ganglion growth cones. *Neuron* 2, 11–20.

Delannet, M., Martin, F., Bossy, B., Cheresh, D. A., Reichardt, L. F., and Duband, J.-L. (1994). Specific roles of the $\alpha V\beta 1$, $\alpha V\beta 3$ and $\alpha V\beta 5$ integrins in avian neural crest cell adhesion and migration on vitronectin. *Development* 120, 2687–2702.

Detwiler, S. R. (1937). Observations upon the migration of neural crest cells, and upon the development of the spinal ganglia and vertebral arches in *Amblystoma*. *Am. J. Anat.* 61, 63–94.

Dunn, G. A. (1982). Contact guidance of cultured tissue cells: A survey of potentially relevant properties of the substratum. *In* ''Cell Behaviour'' (R. Bellairs, A. Curtis, and G. Dunn, Eds.), pp. 247–280. Cambridge Univ. Press, Cambridge.

Dunn, G. A., and Heath, J. P. (1976). A new hypothesis of contact guidance in tissue cells. *Exp. Cell Res.* 101, 1–14.

Duong, T. D., and Erickson, C. A. (1995). Avian neural crest cells produce multiple proteases *in vitro*. *Dev. Biol.* 170, 750a.

DuShane, G. P. (1934). The origin of pigment cells in amphibia. *Science* 80, 620–621.

Epperlein, H. H. (1982). Different distributions of melanophores and xanthophores in early tailbud stages of *Triturus alpestris*. *W. Roux's Arch.* 191, 19–27.

Epperlein, H. H., and Claviez, M. (1982). Changes in the distribution of melanophores and xanthophores in *Triturus alpestris* embryos during their transition from the uniform to banded pattern. *W. Roux's Arch.* 192, 5–18.

Epperlein, H.-H., Halfter, W., and Tucker, R. P. (1988). The distribution of fibronectin and tenascin along migratory pathways of the neural crest in the trunk of amphibian embryos. *Development* 103, 743–756.

Epperlein, H.-H., and Löfberg, J. (1990). The development of the larval pigment patterns in *Triturus alpestris* and *Ambystoma mexicanum*. *Adv. Anat. Embryol. Cell Biol.* 118, 1–101.

Epperlein, H.-H., and Löfberg, J. (1993). The development of the neural crest in amphibians. *Ann. Anat.* 175, 483–499.

Erickson, C. A. (1980). The deformability of BHK cells and polyoma virus-transformed BHK cells in relation to locomotory behaviour. *J. Cell Sci.* 44, 187–200.

Erickson, C. A. (1985). Control of neural crest cell dispersion in the trunk of the avian embryo. *Dev. Biol.* 111, 138–157.

Erickson, C. A. (1993). From the crest to the periphery: Control of pigment cell migration and lineage segregation. *Pigment Cell Res.* 6, 336–347.

Erickson, C. A., and Goins, T. L. (1995). Avian neural crest cells can migrate in the dorsolateral path only if they are specified as melanocytes. *Development* 121, 915–924.

Erickson, C. A., and Perris, R. (1993). The role of cell–cell and cell–matrix interactions in the morphogenesis of the neural crest. *Dev. Biol.* 159, 60–74.

Faassen, A. E., Schrager, J. A., Klein, D. J., Oegema, T. R., Couchman, J. R., and McCarthy, J. B. (1992). A cell surface chondroitin sulfate proteoglycan, immunologically related to CD44, is involved in type I collagen-mediated melanoma cell motility and invasion. *J. Cell Biol.* 116, 521–531.

Gail, M. H., and Boone, C. W. (1971). Density inhibition of motility in 3T3 fibroblasts and their SV40 transformants. *Exp. Cell Res.* 64, 156–162.

Halfter, W., Chiquet-Ehrismann, R., and Tucker, R. P. (1989). The effect of tenascin and embryonic basal lamina on the behavior and morphology of neural crest cells *in vitro*. *Dev. Biol.* 132, 14–25.

Hall, B. K., and Hörstadius, S. (1988). ''The Neural Crest.'' Oxford Univ. Press, New York.

Hara, M., Yaar, M., Tang, A., Eller, M. S., Reenstra, W., and Gilchrest, B. A. (1994). Role of integrins in melanocyte attachment and dendricity. *J. Cell Sci.* 107, 2379–2748.

Harris, A. K., Stopak, D., and Wild, P. (1981). Fibroblast traction as a mechanism for collagen morphogenesis. *Nature* 290, 249–251.

Keller, R. E., Löfberg, J., and Spieth, J. (1982). Neural crest cell behavior in white and dark embryos of *Ambystoma mexicanum:* Epidermal inhibition of pigment cell migration in the white axolotl. *Dev. Biol.* 89, 179–195.

Keller, R. E., and Spieth, J. (1984). Neural crest cell behavior in white and dark larvae of *Ambystoma mexicanum:* Time-lapse cinemicrographic analysis of pigment cell movement in vivo and in culture. *J. Exp. Zool.* 229, 109–126.

Krull, C. E., Collazo, A., Fraser, S. E., and Bronner-Fraser, M. (1995). Segmental migration of trunk neural crest: Time-lapse analysis reveals a role for PNA-binding molecules. *Development* 121, 3733–3743.

Landolt, R. M., Vaughan, L., Winterhalter, K. H., and Zimmermann, D. R. (1995). Versican is selectively expressed in embryonic tissues that act as barriers to neural crest cell migration and axon outgrowth. *Development* 121, 2303–2312.

Lehman, H. E. (1957). The developmental mechanics of pigment pattern formation in the black axolotl, *Amblystoma mexicanum*. *J. Exp. Zool.* 135, 355–386.

Löfberg, J., and Ahlfors, K. (1978). Extracellular matrix organization and early neural crest cell migration in the axolotl embryo. *Zoon* 6, 87–101.

Löfberg, J., Ahlfors, K., and Fällström, C. (1980). Neural crest cell migration in relation to extracellular matrix organization in the embryonic axolotl trunk. *Dev. Biol.* 75, 148–167.

Löfberg, J., Nynäs-McCoy, A., Olsson, C., Jönsson, L., and Perris, R. (1985). Stimulation of initial neural crest cell migration in the axolotl embryo by tissue grafts and extracellular matrix transplanted on microcarriers. *Dev. Biol.* 107, 442–459.

Mackie, E. J., Halfter, W., and Liverani, D. (1988). Induction of tenascin in healing wounds. *J. Cell Biol.* 107, 2757–2767.

Newgreen, D. F. (1989). Physical influences on neural crest cell migration in avian embryos: Contact guidance and spatial restriction. *Dev. Biol.* 131, 136–148.

Northcutt, R. G. (1992). Distribution and innervation of lateral line organs in the axolotl. *J. Comp. Neurol.* 325, 95–123.

Northcutt, R. G., Brändle, K., and Fritzsch, B. (1995). Electroreceptors and mechanosensory lateral line organs arise from single placodes in axolotls. *Dev. Biol.* 168, 358–373.

Northcutt, R. G., Catania, K. C., and Criley, B. B. (1994). Development of lateral line organs in the axolotl. *J. Comp. Neurol.* 340, 480–514.

Oakley, R. A., Lasky, C. J., Erickson, C. A., and Tosney, K. W. (1994). Glyconjugates mark a transient barrier to neural crest migration in the chicken embryo. *Development* 120, 103–114.

Olsson, L., and Löfberg, J. (1992). Pigment pattern formation in larval ambystomatid salamanders: *Ambystoma tigrinum tigrinum*. *J. Morphol.* 211, 73–85.

Olsson, L., Stigson, M., Perris, R., Sorrell, J. M., and Löfberg, J. (1996). Distribution of keratan sulphate and chondroitin sulphate in wild type and white mutant axolotl embryos during neural crest cell migration. *Pigment Cell Res.*, in press.

Paddock, S. W., and Dunn, G. A. (1986). Analysing collisions between fibroblasts and fibrosarcoma cells: Fibrosarcoma cells show an active invasionary response. *J. Cell Sci.* 81, 163–187.

Parichy, D. M. (1996a). Salamander pigment patterns: How can they be used to study developmental mechanisms and their evolutionary transformation? *Int. J. Dev. Biol.*, in press.

Parichy, D. M. (1996b). Pigment patterns of larval salamanders (Ambystomatidae, Salamandridae): The role of the lateral line sensory system and the evolution of pattern-forming mechanisms. *Dev. Biol.* 174, 265–282.

Perris, R., and Johansson, S. (1987). Amphibian neural crest cell migration on purified extracellular matrix components: A chondroitin sulfate proteoglycan inhibits locomotion on fibronectin substrates. *J. Cell Biol.* 105, 2511–2521.

Perris, R., Löfberg, J., Fällström, C., von Boxberg, Y., Olsson, L., and Newgreen, D. F. (1990). Structural and compositional divergencies in the extracellular matrix encountered by neural crest cells in the white mutant axolotl. *Development* 109, 533–551.

Qian, F., Vaux, D. L., and Weissman, I. L. (1994). Expression of the integrin $\alpha 4\beta 1$ on melanoma cells can inhibit the invasive stage of metastasis formation. *Cell* 77, 335–347.

Raible, D. W., and Eisen, J. S. (1994). Restriction of neural crest cell fate in the trunk of the embryonic zebrafish. *Development* 120, 495–503.

Ranscht, B., and Bronner-Fraser, M. (1991). T-cadherin expression alternates with migrating neural crest cells in the trunk of the avian embryo. *Development* 111, 15–22.

Riou, J.-F., Alfandari, D., Eppe, M., Tacchetti, C., Chiquet, M., Boucaut, J. C., Thiery, J.-P., and Levi, G. (1991). Purification and partial characterization of *Xenopus laevis* tenascin from the XTC cell line. *FEBS Lett.* 279, 346–350.

Rovasio, R. A., Delouvee, A., Yamada, K. M., Timpl, R., and Thiery, J. P. (1983). Neural crest cell migration: Requirements for exogenous fibronectin and high cell density. *J. Cell Biol.* 96, 462–473.

Sato, A. (1976). Electron microscopic study of the developing lateral-line organ in the embryo of the newt, *Triturus pyrrhogaster*. *Anat. Rec.* 186, 565–584.

Seftor, R. E. B., Seftor, E. A., Gehlsen, K. R., Stetler-Stevenson, W. G., Brown, P. D., Ruoslahti, E., and Hendrix, M. J. C. (1992). Role of the $\alpha_v\beta_3$ integrin in human melanoma cell invasion. *Proc. Natl. Acad. Sci. USA* 89, 1557–1561.

Selleck, M. A. J., Scherson, T. Y., and Bronner-Fraser, M. (1993). Origins of neural crest cell diversity. *Dev. Biol.* 159, 1–11.

Serbedzija, G. N., Bronner-Fraser, M., and Fraser, S. E. (1994). Developmental potential of trunk neural crest cells in the mouse. *Development* 120, 1709–1718.

Shaffer, H. B. (1993). Systematics of model organisms: the laboratory axolotl, *Ambystoma mexicanum*. *Syst. Biol.* 42, 508–522.

Smith, M., Hickman, A., Amanze, D., Lumsden, A., and Thorogood, P. (1994). Trunk neural crest origin of caudal fin mesenchyme in the zebrafish *Brachydanio rerio*. *Proc. R. Soc. London B* 256, 137–145.

Smith, S. C., Lannoo, M. J., and Armstrong, J. B. (1988). Lateral-line neuromast development in *Ambystoma mexicanum* and a comparison with *Rana pipiens*. *J. Morphol.* 198, 367–379.

Smith, S. C., Lannoo, M. J., and Armstrong, J. B. (1990). Development of the mechanoreceptive lateral-line system in the axolotl: Placode specification, guidance of migration, and the origin of neuromast polarity. *Anat. Embryol.* 182, 171–180.

Spence, S. G., and Poole, T. J. (1994). Developing blood vessels and associated extracellular matrix as substrates for neural crest migration in Japanese quail, *Coturnix coturnix japonica*. *Int. J. Dev. Biol.* 38, 85–98.

Stetler-Stevenson, W. G., Aznavoorian, S., and Liotta, L. A. (1993). Tumor cell interactions with the extracellular matrix during invasion and metastasis. *Annu. Rev. Cell Biol.* 9, 541–573.

Stone, L. S. (1933). The development of lateral-line sense organs in amphibians observed in living and vital-stained preparations. *J. Comp. Neurol.* 57, 507–540.

Stone, L. S. (1938). Further experimental studies of the development of lateral-line sense organs in amphibians observed in living preparations. *J. Comp. Neurol.* 68, 83–115.

Tang, A., Eller, M. S., Hara, M., Yaar, M., Hirohashi, S., and Gilchrest, B. A. (1994). E-cadherin is the major mediator of human

melanocyte adhesion to keratinocytes *in vitro*. *J. Cell Sci.* 107, 983–992.

Thiery, J. P., Duband, J. L., and Delouvée, A. (1982). Pathways and mechanisms of avian neural crest cell migration and localization. *Dev. Biol.* 93, 324–343.

Thomas, L., Byers, H. R., Vink, J., and Stamenkovic, I. (1992). CD44H regulates tumor cell migration on hyaluronate-coated substrate. *J. Cell Biol.* 118, 971–977.

Thomas, L. A., and Yamada, K. M. (1992). Contact stimulation of cell migration. *J. Cell Sci.* 103, 1211–1214.

Tickle, C., and Trinkaus, J. P. (1976). Observations on nudging cells in culture. *Nature* 261, 413.

Tickle, C. A., and Trinkaus, J. P. (1973). Change in surface extensibility of *Fundulus* deep cells during early development. *J. Cell Sci.* 13, 721–726.

Tosney, K. W., Dehnbostel, D. B., and Erickson, C. A. (1994). Neural crest cells prefer the myotome's basal lamina over the sclerotome as a substratum. *Dev. Biol.* 163, 389–406.

Tucker, R. P. (1986). The role of glycosaminoglycans in anuran pigment cell migration. *J. Embryol. Exp. Morphol.* 92, 145–164.

Tucker, R. P., Edwards, B. F., and Erickson, C. A. (1985). Tension in the culture dish: Microfilament organization and migratory behavior of quail neural crest cells. *Cell Motility* 5, 225–237.

Tucker, R. P., and Erickson, C. A. (1984). Morphology and behavior of quail neural crest cells in artificial three-dimensional extracellular matrices. *Dev. Biol.* 104, 390–405.

Tucker, R. P., and Erickson, C. A. (1986a). The control of pigment cell pattern formation in the California newt, *Taricha torosa*. *J. Embryol. Exp. Morphol.* 97, 141–169.

Tucker, R. P., and Erickson, C. A. (1986b). Pigment cell pattern formation in *Taricha torosa:* The role of the extracellular matrix in controlling pigment cell migration and differentiation. *Dev. Biol.* 118, 268–285.

Twitty, V. C., and Niu, M. C. (1948). Causal analysis of chromatophore migration. *J. Exp. Zool.* 108, 405–437.

Wehrle-Haller, B., and Chiquet, M. (1993). Dual function of tenascin: Simultaneous promotion of neurite growth and inhibition of glial migration. *J. Cell Sci.* 106, 597–610.

Winklbauer, R. (1989). Development of the lateral line system in *Xenopus*. *Progr. Neurobiol.* 32, 181–206.

Zambruno, G., Marchisio, P. C., Melchiori, A., Bondanza, S., Cancedda, R., and De Luca, M. (1993). Expression of integrin receptors and their role in adhesion, spreading and migration of normal human melanocytes. *J. Cell Sci.* 105, 179–190.

Received for publication October 25, 1995
Accepted January 4, 1996